Substrate temperature and strain during sputter deposition of aluminum on cast borosilicate glass in a Gemini Observatory coating chamber

Jacques Sebag[1], John Andrew[1], Douglas Neill[1], and Michael Warner[2]
[1]National Optical Astronomy Observatory, 950 North Cherry Avenue, Tucson, Arizona 85719, USA
[2]Cerro Tololo Inter-American Observatory, Casilla 603, La Serena, Chile
Received 15 March 2010; Published 18 August 2010
Synopsis by Blake Coughenour

Abstract: Temperature and strain measurements obtained during coating of spin-cast borosilicate samples are presented here with an analysis of these results. These tests were performed for the Large Synoptic Survey Telescope (LSST) project to verify the possible use of sputtering deposition of optical coating on its large 8:4 m diameter primary–tertiary mirror. Made of spin-cast borosilicate glass, the working stress of the mirror's nonpolished surfaces is 100 psi (0.69 MPa), resulting in a local temperature difference limit of 5 °C. To ensure representative environmental conditions, the tests were performed in the Gemini Observatory coating chamber located in Hawaii, whose design was utilized to develop the LSST coating chamber design. In particular, this coating chamber is equipped with linear magnetrons built with cooled heat shields directly facing the mirror surface. These measurements have demonstrated that it will be safe for the LSST to use a magnetron sputtering process for coating its borosilicate primary–tertiary.

1. Introduction

This report summarizes the feasibility of coating the Large Synoptic Survey Telescope (LSST) 8.4 m diameter primary-tertiary borosilicate (BSG) mirror in silver and aluminum using a sputtering technique instead of a conventional aluminum evaporation technique. The added benefits would be higher reflectivity and durability than bare aluminum resulting in increased throughput over a longer period of time. However, until now sputter coating of silver mixtures has only been performed on large astronomical mirrors made of Zerodur or ULE. This is because the sputtering process bombards a small area of the substrate surface with ions generating a localized temperature difference that low expansion glasses can endure. The borosilicate glass will have to withstand the strain created by this heat flux without failing structurally.

Sputter coating is preferred for heavy use astronomical mirrors because it can provide greater layer thickness and coating uniformity than that provided by conventional evaporation techniques. In the process of sputtering, the coating chamber is backfilled with a continuous flow of argon gas to establish a glow discharge. The positive ions from the plasma are accelerated by strong electric fields and bombard a condensed-matter target that acts as the cathode. This target heats up and must be actively cooled. The ion bombardment ejects particles from the target that impact the substrate generating a small heat load. Although the heat load from particle flux is small, substantial heating of the substrate is possible because convection is negligible in the vacuum chamber.

The Gemini Observatory operates two large coating chambers (one in Hawaii and one in Chile). The sputtering system they use utilizes a direct-current system that provides active cooling to the target. Using a single DC magnetron combined with this direct cooling operation reduces the heat transfer to the substrate.

Table 1. Borosilicate Glass Characteristics

Young's Modulus (E)	58.6 GPa
Thermal Diffusivity (D)	1.11 x10^{-7} m^2/s
CTE (α)	2.8 ppm/K
Specific Heat (c)	710 J/kg °C

The LSST mirror is a cast borosilicate mirror with a 28mm thick faceplate. The relevant material properties of borosilicate are provided in table 1. The material has both a significantly higher coefficient of thermal expansion and a lower strength making it more susceptible to thermal damage than Zerodur or ULE. The typical breaking strength of borosilicate is approximately 2000 psi (13.8 MPa). For the large borosilicate honeycomb blanks cast in the Steward Observatory Mirror Lab, the roughness of the interior surfaces combined with residual stresses yields a maximum tensile stress of 100 psi (0.7 MPa), which further increases to 300 psi (2.1 MPa) on the polished surface. This tensile stress threshold can be used to estimate the maximum allowable temperature gradient in any direction across the mirror or through its thickness.

Applying radial symmetry to a polished faceplate over a given honeycomb, we can model the stress as a radial beam when a top-down thermal gradient is applied to the faceplate with the edges constrained. This thermal gradient is found by solving the following equation:

$$\sigma_{tensile} \approx \alpha E \Delta T \rightarrow \Delta T \approx \frac{\sigma_{tensile}}{E\alpha} = 4.26^{\circ}C$$

Those most familiar with the mechanical properties of these mirrors have calculated a slightly higher maximum allowable thermal gradient of 5 ºC, which will be used in subsequent validation analysis of this experiment.

In this paper, the authors examine the heat load on samples of borosilicate glass using the Gemini North Telescope coating chamber. They conclude that sputter coating with be safe for large borosilicate mirrors.

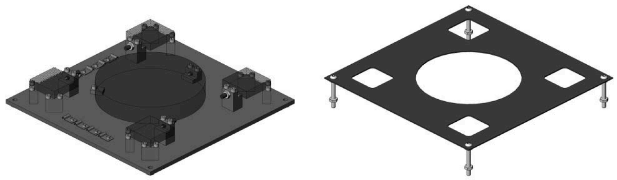

(a) (b)

Fig. 1. Test plate with (a) samples and (b) reusable shield plate

2. Coating Test Configuration

Since these tests would seek to discretely and accurately measure the temperature change of borosilicate glass, of particular interest was the direct-cooling linear magnetron sputtering configuration in the Gemini chamber used in conjunction with a cooled uniformity mask located in front of the target. This mask is used to control the coating layer thickness uniformity while the mirror rotates below the magnetron to compensate for the mirror's radial linear speed variation. There was also a cooled shutter between the target and a reusable shield plate to control precisely the area to be coated on the mirror to obtain uniform coating thickness (Fig. 1).

A water coolant flow provided an input temperature of 9 °C. During coating, the output temperature of the coolant would climb to 21 °C, which represents an additional ooling load equal to 53 kW. For these tests, the distance between the mask and the sample was approximately 25 mm while the target was positioned another 75 mm above the mask. These distances were chosen to match the expected configuration in the LSST coating chamber.

The Gemini chamber was built with the capability of sputter depositing aluminum, and aluminum was chosen for these thermal tests because it requires slightly more power during deposition and represents a worst-case thermal scenario. Moreover, LSST may also deposit aluminum on its mirrors. In the test, the chamber's maximum power of 40 kW was intended to be used to deposit a 100nm layer of aluminum in one pass under the magnetron. Since only 10 kW was possible at the time of the tests, the radial speed of the mirror was slowed to achieve the same layer thickness. Throughout the experiment, temperature and strain were measured using thermocouples and strain gauges with a small cross-section to minimize conduction. Temperature modeling was used to extrapolate these results to higher power levels and different deposition times.

Three different types of materials were tested in the process to verify the models: float, pyrex, and borosilicate glass. In this summary, only the results from the 28 mm thick borosilicate samples will be examined as this test substrate and thickness most closely match the properties of large mirror surfaces in question. It will suffice to say that the other materials verify the thermal models.

3. Temperature Test Results and Models

For the 28mm thick borosilicate sample, the measured temperature on the top surface increased quickly by 2.3 ºC in 50 s, and then decreased by 1.3 ºC in 250 s to reach equilibrium. On the back surface, the temperature began rising after the top surface temperature had reached its maximum and continued to increase slowly, 0.8 ºC in 250 s to reach the same equilibrium temperature as the front surface. The change in mean temperature through the thickness can be predicted by an energy balance equation:

$$Q - A\sigma\varepsilon(T_1^4 - T_2^4) = mc\frac{dT}{dt} \tag{1}$$

where Q is the substrate heat load in watts entering the sample from the sputtering process, A is the radiative area in m^2, σ is the Boltzmann constant ($W/m^2\ K^4$), ε is the emissivity, m is the mass in kg, c is the specific heat of the substrate (J/kg°C), T is the mean temperature of the sample, T_1 the temperature of the exposed surface of the sample, T_2 is the ambient temperature, and t is the coating time (s). The second term in (1) is the energy emitted by radiation from the sample and the third term is the increase in thermal energy. Because the energy emitted from the sample through radiation was minimal (25mW), the front and back surface temperatures were set equal to the mean temperature to simplify the calculations.

During the coating, a significant temperature gradient develops through the 28mm thickness, and the front and back surface temperature change at a different rate. The temperature as a function of depth "x" can be predicted by the unsteady energy balance equation:

$$T_x - T_i = 2\frac{Q}{A}\frac{\sqrt{Dt\pi}}{k}\exp\left(\frac{-x^2}{4Dt}\right) - \frac{Qx}{Ak}\left[1 - erf\left(\frac{x}{2\sqrt{Dt}}\right)\right] \tag{2}$$

where ρ is the density (kg/m3), k is the thermal conductivity (W/m°C), D is the thermal diffusivity, T_x is the temperature as a function of depth, T_i is the initial temperature, and x is the distance from the front surface. Calculated results of temperature changes are shown in Table 2 while graphical results are shown in Figure 2.

After the coating, since the samples are no longer experiencing a heat flux and radiation losses are negligible, the decay of the thermal gradient is governed entirely by conduction. This decay model can be solved using the thermal gradient by discretizing the substrate throughout its thickness and solving iteratively.

Table 2. Temperature Results for 28mm Borosilicate Sample

Measured T increase on top during coating	2.3 °C (50s)
Measured T decrease on top after coating	1.3 °C (250s)
Measured T increase on back during coating	0.8 °C (250s)
Predicted mean ΔT increase after coating	0.74 °C
Predicted front-to-back ΔT difference	2.0 °C

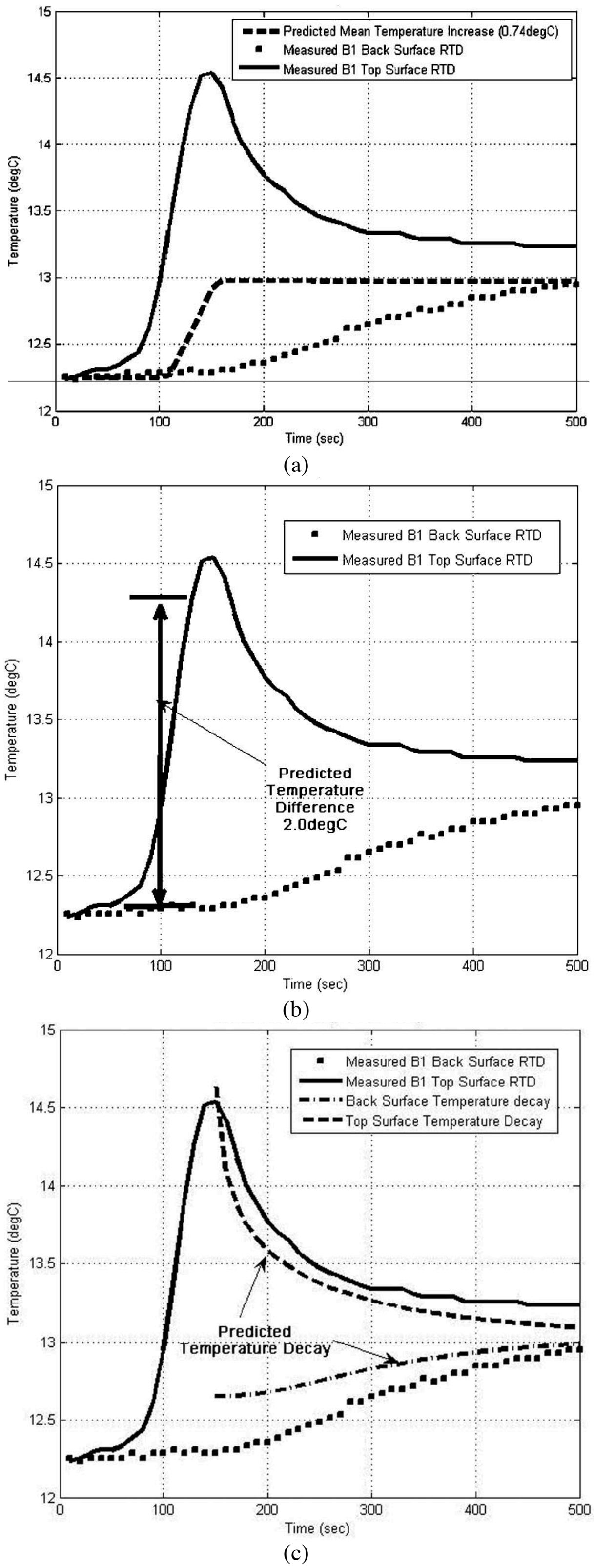

Fig. 2. Comparison of measured and predicted mean temperature increase (a), measured and predicted temperature difference (b), and measured and predicted thermal decay (c) all shown for the 28mm thick borosilicate glass sample

The thermal models yield good agreement with the measured data and so they are then used to extrapolate the measured results to a set of different coating conditions. For the LSST mirror, the desired layer thickness is 100 nm obtained in one pass below the magnetrons. During these tests, the averaged coating thickness was 69 nm. To increase the thickness to 100 nm, the rotational speed of the mirror could be decreased or the power can be increased to 20, 30 or 40kW while maintaining the same rotational speed.

Reducing the rotational speed to 0.74 mm/s from 1.13 mm/s (at the 2.6m sample radius) should yield a 100 nm average thickness. This corresponds to an increased deposition coating time of 68 s from 47 s for a 10 kW power level. Using (1), this increase in time results in a 2.2 °C predicted temperature difference between the front and back surfaces. Being below 5 °C, this result shows it would be safe to coat the LSST mirror with this process.

Increasing the power might be preferred because higher power levels have been shown to produce coatings with better reflectance performances. With this procedure, the coating rate is increased and the 100 nm layer thickness is achieved quicker with a faster rotational speed. Using (2), the predicted front-to-back temperature difference is calculated and shown in Table 3. All of the resulting temperatures show that the range should not exceed the 5 °C safe limit even for the highest power case of 40 kW.

Table 3. Predicted Impact of Power Change on BSC Sample

Magnetron Power (kW)	10	20	30	40
Coating Duration (s)	47	34	23	17
Rotational Speed (rph)	0.25	0.32	0.48	0.64
Front-to-Back ΔT (°C)	2.0	3.2	3.9	4.5

4. Maximum Stress Prediction from Thermal Models

These models can be used to compute a predicted maximum stress due to thermal strain assuming the thermal expansion is completely restrained. In this case the thermal strain ε_{Th} and mechanical strain ε_M are equal in magnitude and opposite in direction and given by:

$$\varepsilon_{Th} = \alpha \times \Delta T \tag{3}$$

in the entirely constrained case, the stress σ is given by the product of the strain and elastic modulus E of BSG:

$$\sigma = \varepsilon_M \times E = -\varepsilon_{Th} \times E \tag{4}$$

For these tests, the maximum theoretically possible stress occurs for the 40 kW power case where it reaches a peak value just above 100 psi in the last ~2 s of deposition. In reality, the actual stress from constraint comes from only about 50% of the total thermal strain, resulting in a maximum surface stress of 50 psi (0.34 MPa). This is below the 300 psi (2.1 MPa) limit set for the polished surfaces of the large borosilicate mirror.

5. Strain Measurements During Coating Tests

The BSG samples were instrumented with strain gauges on the back surfaces to measure mechanical strain directly. Strain gauges on the front surface failed possibly due to interference with the magnetron. One BSG sample (on Plate B) had a polished surface representative of the LSST optical surface and had a uniform thickness of 28 mm. The other BSG sample (on Plate C) had a rough front surface more representative of irregularities in the nonpolished surfaces. This sample also had a variable radial thickness decreasing from 28 mm at the edge to 8 mm at the center along a spherical shape on the uncoated backside.

Throughout the tests, the maximum raw strain values obtained for the BSC sample were 6 ppm (μstrain) on plate B and 12 ppm on plate C. The strain gauges are resistive sensors whose electrical resistance varies with temperature. To compute real total strain, the raw signal must be corrected for this thermal output using calibration coefficients from the manufacturer. Applying the thermal output correction, the total strain for the BSC sample becomes 1.3 ppm on plate B and 4 ppm on plate C.

The strain gauges measure the total strain ε, the sum of the thermal strain and mechanical strain. The thermal strain (3), is the inherent expansion of the glass from the increase in temperature. The measured temperature change on the back surface of the BSG sample is equal to 0.8 K for plate B and 2 K for plate C, giving thermal strain values of 2.24 ppm and 5.6 ppm respectively. The mechanical strain is found by subtracting the thermal strain from the total strain measured by the strain guages. After subtraction, the mechanical strain reaches -0.9 ppm for plate B and -1.6 ppm for place C. The negative sign means the mechanical strain is in compression. The stress is the product of the mechanical strain and the Young's modulus for borosilicate glass. All of these results are summarized in Table 4 below.

Table 4. Back-Surface Stress from Measured Strain

BSG Sample	Plate B	Plate C
Thermal Strain (ppm)	2.24	5.6
Total Strain (ppm)	1.3	4
Mechanical Strain (ppm)	-0.94	-1.6
Stress (psi)	-8	-14

The computed stress on the back surface of 14 psi (0.1 MPa) is well below the 100 psi tensile stress limit. The stress on the front surface was not found experimentally due to magnetron interference, yet it can be estimated using the temperature gradient. Since the temperature increase is concentrated on the top surface and it rises 2 or 3 times greater than on the back surface, the stress on the top surface should be of order 3 times larger than the back surface stress according to the moment balance and superposition principles.

We expect that for the sample of uniform thickness, the actual stress on the top surface would around 24 psi (0.16 MPa) for the 10 kW configuration. This result is in good agreement with the predicted actual stress of 23 psi estimated above using the temperature model. For the 40 kW configuration, this same extrapolation would produce a top surface actual stress of 54 psi which is well within the safe polished surface stress limit of 300 psi (2.1 MPa) and the tensile limit of 100 psi (0.7 MPa) for the large cast borosilicate mirrors.

6. Conclusions

A cast borosilicate mirror can be safely coated with sputtering. The measured maximum temperature variation between the front and back surfaces of the 28mm thick BSG sample where within the safe limits of cast borosilicate for a coating thickness of 69 nm. Utilizing the validated temperature models, variations in power, thickness, coating times, and mechanical stress coupling showed that in every case the resulting temperatures were within the safe limit of 5 ºC and the resulting stresses were below 100 psi (0.7 MPa) throughout the glass.

References

1. V. Krabbendam, "The Large Synoptic Survey Telescope concept design overview," Proc. SPIE 7012, 701205 (2008).
2. J. M. Hill, J. R. P. Angel, R. D. Lutz, B. H. Olbert, and P. A. Strittmatter, "Casting the first 8:4 m borosilicate honeycomb mirror for the Large Binocular Telescope," Proc. SPIE 3352, 172–181 (1998).
3. J. Sebag, V. Krabbendam, G. Poczulp, D. Neill, T. Vucina, and M. Boccas, "LSST reflective coating studies," Proc. SPIE 6273, 62730X (2006).
4. M. Boccas, T. Vucina, C. Araya, E. Vera, and C. Ah'Hee, "Coating the 8 m Gemini telescopes with protected silver," Proc. SPIE 5494, 239–253 (2004).
5. M. Schneermann, M. Groessi, U. Nienaber, E. Ettlinger, J. A. Spiteri, and H. Clow, "Design and performance of the VLT 8 meter coating unit," Proc. SPIE 2871, 136–144 (1997).
6. B. Atwood, D. Pappalardo, T. O'Brien, J. M. Hill, J. Mason, R. Belville, D. Steinbrecher, D. Brewer, E. Teiga, B. Sabol, J. Howard, and L. Miglietta, "The aluminizing system for the 8.4 meter diameter LBT primary mirrors," Proc. SPIE 6273, 62730T (2006).
7. J. A. Thornton and J. E. Greene, "Sputter deposition processes," Handbook of Deposition Technologies for Films and Coatings, 2nd ed. (Noyes Publications, 1994), pp. 249–319.
8. W. B. Davison, J. T.Williams, and J. M. Hill, "Handling 20 tons of honeycomb mirror with a very gentle touch," Proc. SPIE 3352, 216–224 (1998).
9. J. M. Hill, J. R. P. Angel, and B. Olbert, "Rules for handling large borosilicate honeycomb mirrors," Columbus Project Technical Memo UA-92-05 (Steward Mirror Lab, 1992).
10. J. R. Plaisted, G. McDonough, and G. Roche, "Effects of the anode configuration on substrate heating in dual magnetron sputtering," White paper SL-WHITE3-270-01 (Advanced Energy Industries Corporation, 2001).
11. Vishay Micro-Measurements, "Strain gage rosettes," Technical Note TN-515 (Vishay Micro-Measurements, 2008)